# Packaging and Qualification of Single Photon Counting Avalanche Photodiode Focal Plane Arrays

Joseph E. Funk, Gary M. Smith, K. Alex McIntosh, Joseph P. Donnelly,
Michael A. Brattain, Albert C. Ruff, and Simon Verghese
MIT Lincoln Laboratory, 244 Wood Street, Lexington, MA USA 02420

## ABSTRACT

Avalanche Photodiode (APD) photon counting arrays are finding an increasing role in defense applications in laser radar and optical communications. As these system concepts mature, the need for reliable screening, test, assembly and packaging of these novel devices has become increasingly critical. MIT Lincoln Laboratory has put significant effort into the screening, reliability testing, and packaging of these components. To provide rapid test and measurement of the APD devices under development, several custom parallel measurement and Geiger-mode (Gm) aging systems have been developed.

Another challenge is the accurate attachment of the microlens arrays with the APD arrays to maximize the photon detection efficiency. We have developed an active alignment process with single µm precision in all six degrees of free-space alignment. This is suitable for the alignment of arrays with active areas as small as 5 µm. Finally, we will discuss a focal plane array (FPA) packaging qualification effort, to verify that single photon counting FPAs can survive in future airborne systems.

**Keywords:** single photon detector, photon imager, microlens alignment, avalanche photodiodes, reliability, packaging

## 1. INTRODUCTION

Single photon counting GmAPD arrays are finding an increasing role in Government applications such as laser radar and deep-space optical communications systems [1,2]. MIT Lincoln Laboratory has committed significant resources to the reliability testing, optical optimization, packaging and Highly Accelerated Stress Screening (HASS) of these assemblies.

## 2. RELIABILITY SCREENING

During the development cycle of avalanche photodiode arrays, the need exists to have the capability to rapidly quantify and measure the results of a specific fabrication and/or process change. To that end, MIT Lincoln Laboratory has developed several systems to automatically characterize and age APDs with a standardized data format for analysis. Additionally, these systems are an integral part of the screening process for the qualification of components. For each fabrication run, a sample set of arrays or test structures can be wire bonded into a Dual Inline Package (DIP) for an automated set of tests. From these comprehensive tests, a decision can be made as to the viability of a particular lot for use as a system component.

### 2.1 APD Aging Systems

MIT Lincoln Laboratory has developed several APD characterization systems that are based on a custom designed Printed Circuit Board (PCB) that provide independent DC bias voltage and AC over bias supplies for each of the 39 channels (see Fig. 1). The PCBs are housed in a thermal chamber that allows for APD characterization across a wide temperature range (-75°C to 80°C) and is capable of fully automated, *in situ* parallel aging and testing of APDs.

This work has been sponsored by the U.S. Defense Advanced Research Project Agency under Air Force contract number FA8721-05-C-0002. The opinions, interpretations, conclusions, and recommendations are those of the authors and are not necessarily endorsed by the United States Government. *- Approved for Public Release, Distribution Unlimited*

Advanced Photon Counting Techniques III, edited by Mark A. Itzler, Joe C. Campbell,
Proc. of SPIE Vol. 7320, 73200S · © 2009 SPIE · CCC code: 0277-786X/09/$18 · doi: 10.1117/12.821294

Each PCB has 39 programmable onboard DC supplies capable of supplying 1mA of current from 1 – 150 Vdc in 100 µA increments. The AC over-bias supply also has 39 independently programmable channels and operating from 1 – 14 Vdc.

APD aging and characterization currently consists of the automated test and acquisition of Dark Count Rate (DCR), dark current, current / voltage characterization, and after pulsing measurement. APD event detection can either be monitored from the anode or cathode side of the APD circuit; although when monitoring from the low side (array common anode), only one device can be accurately measured at a time. The experimental data have shown that these systems are capable of a high charge flow acceleration of over 1000X as compared to more typical array operation on a CMOS Read Out Integrated Circuit (ROIC) [2].

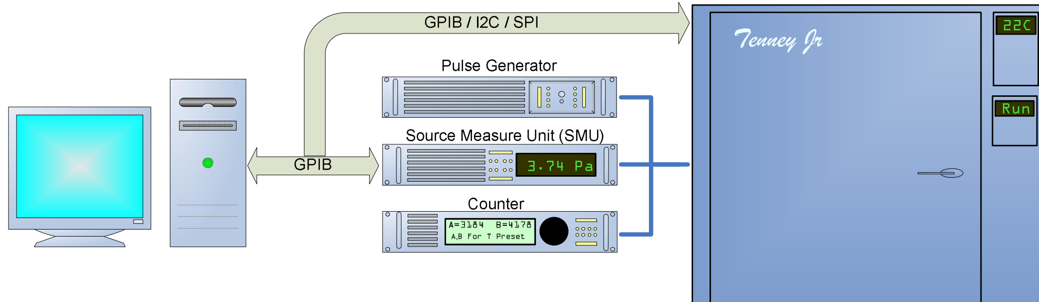


Figure 1. APD test system.

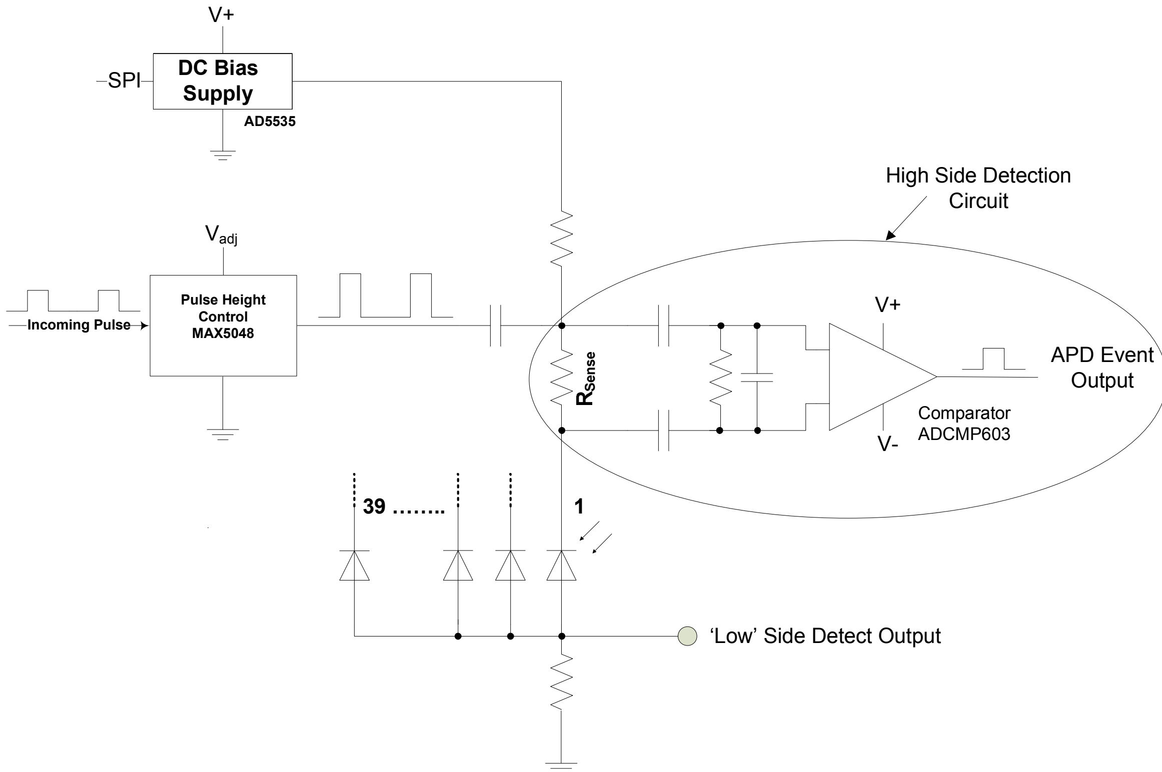


Figure 2. Simplified schematic of the APD test circuit. This would represent one of 39 identical circuits on the parallel aging PCB. All relevant elements of this circuit are programmable.

All APD aging systems are fully automated and capable of unattended operations for an extended length of time. This allows for an uninterrupted test cycle resulting in uniform and repeatable data. The test sequence is defined using a standardized template that specifies the test types and all aging parameters. All resultant data are automatically recorded and formatted for later analysis. An example of the capabilities of the system can be seen in (see Fig. 3), which shows the results of DCR measurements taken over a wide temperature range.

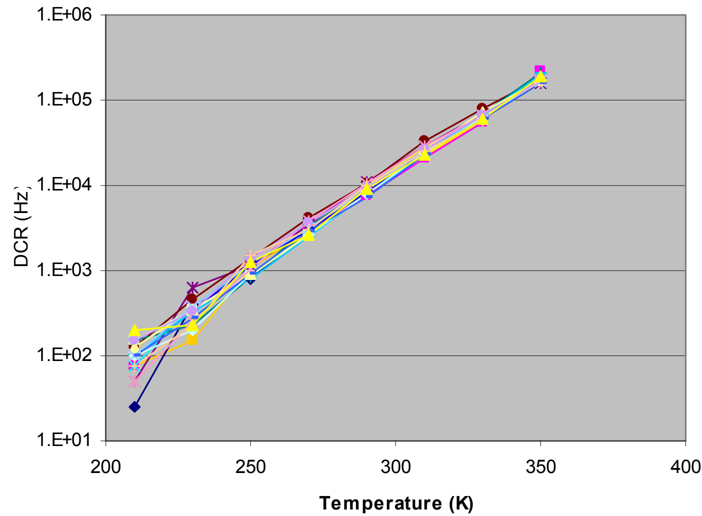


Figure 3. Example data showing the effect of temperature on DCR for 20 µm diameter APDs.

## 3. MICROLENS ALIGNMENT & ATTACHMENT

In both LADAR and laser communications systems, increased optical coupling efficiencies are beneficial to the overall system performance. Microlens arrays have been employed to increase the fill factor and subsequent optical sensitivity of the APD assembly. In certain systems, the diameters of the APDs approach 10 µm requiring alignment and attachment methods that are capable of achieving accuracies of ≤1 µm. MIT Lincoln Laboratory has developed an active alignment process and dedicated alignment system that uses the APD structure to provide direct, real time feedback to the alignment process. The accuracy of this process is integral to achieving a high PDE for the APD / ROIC assemblies (see Fig. 4).

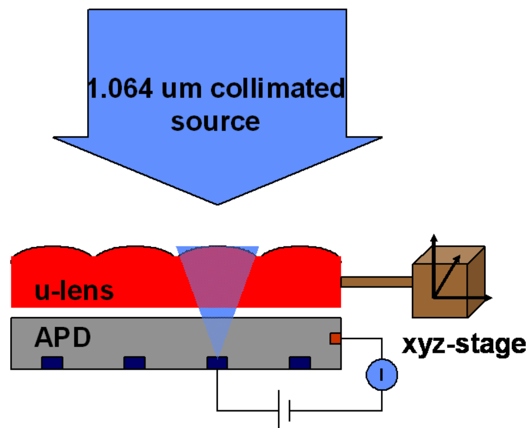


Figure 4. Simplified diagram of the microlens alignment system.

### 3.1 Microlens Alignment

Two methods of active alignment have been developed; the first method includes the addition to the normal array structure of independent corner diodes which are isolated electrically from the main APD array (see Fig. 5). The corner diodes are independently biased below breakdown and monitored in a real-time basis for changes in photocurrent during the alignment process. While monitoring the photocurrent, the APD array is adjusted in all six degrees of freedom with movements as small as 100 nm. Overall, this method yields the best results, resulting in a near perfect alignment with accuracies demonstrated at less than 1 µm (see Fig. 6a).

The second method involves applying a bias voltage to the whole APD array; this includes modestly biasing all APDs in the array. Using the sum of all the photocurrents, the microlens array is accurately positioned over the APD array. It has been found that the best accuracy that can be reliably achieved is +/- 2 µm (see Fig. 6b). This method, while accurate, can be problematic if there are defective APDs in the array (i.e. shorted or high leakage current). Since the whole array is being used for the alignment process, a single high leakage current diode can result in a higher potential error in the alignment.

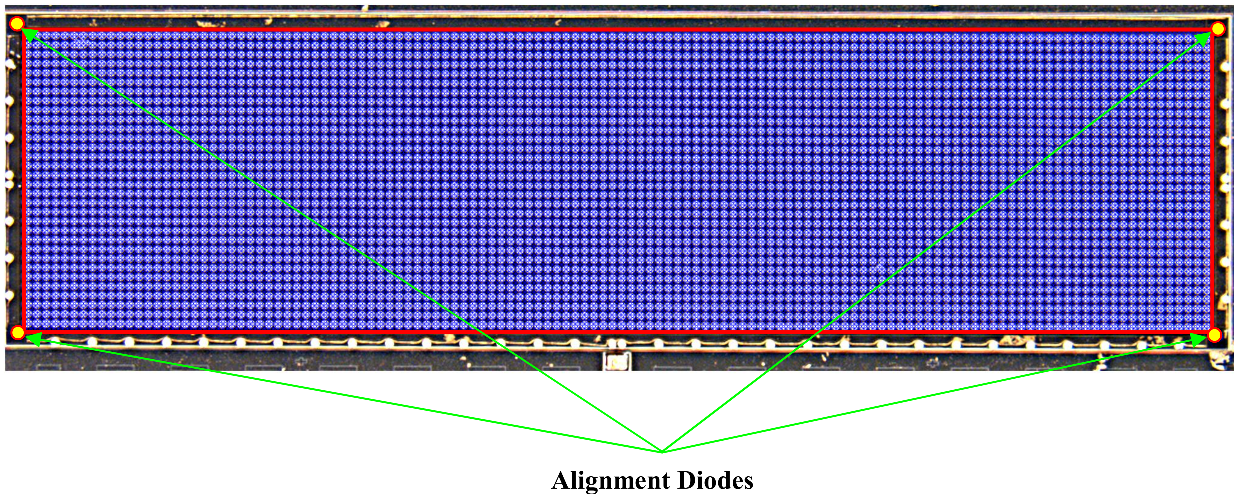


Figure 5. 128x32 APD array with 4 corner alignment diodes. The main 128x32 array is outlined in red with the 4 independent alignment diodes in yellow. The array pitch is 50 µm.

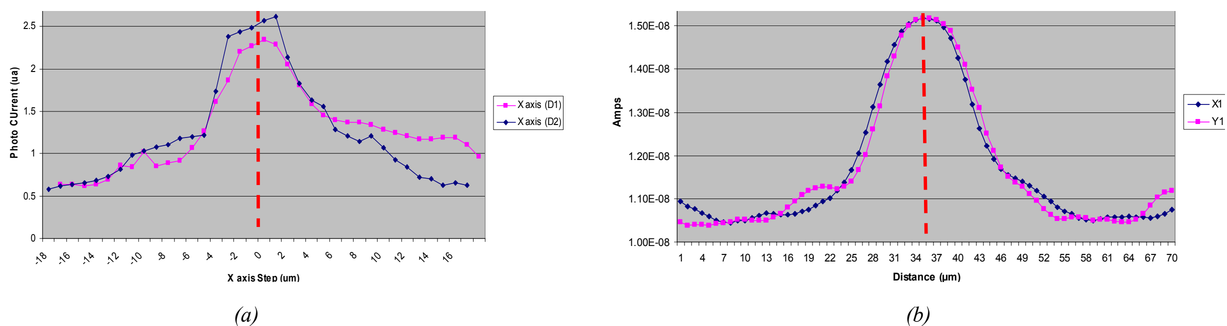


Figure 6. Examples of both the independent (*a*) and whole array (*b*) alignment data.

### 3.2 Microlens Attachment

Once alignment has been achieved, the challenge is to affix the APD array to the microlens array while maintaining the precise position as defined by the initial alignment process. To accomplish this, the use of a two-part thermoplastic epoxy adhesive has been employed. The current method uses a series of 100 µm diameter adhesive dots placed around the periphery of the APD array, after which the microlens alignment is verified and monitored throughout the process of adhesive cross linking and curing.

After the *in situ* monitoring of the curing process (typically 24 hours), the assembly is removed and placed into a vacuum oven for the final cure cycle. The purpose of curing the adhesive at a higher temperature is to achieve a glass transition point (Tg) that is compatible with other process steps. During the higher temperature cure cycle it is imperative to keep the temperature ramp rate well under any potential cross linking phase change. This has been the key to maintaining the alignment during the high temperature cure cycle. Additionally, the need for a higher Tg point is seen later in the assembly process of the APD FPA.

The process as currently defined requires that the ROIC/APD / microlens assembly be soldered onto the TEC after the microlens has been aligned and attached. If the Tg point were significantly lower than the temperatures used during the solder step, the potential exists for drift in the microlens alignment due to a subtle phase change as a result of the rapid heating that is incurred during the solder process.

As an example, typically the heating ramp rate does not exceed 0.1°C/min for Tra-Con F118 two part thermoplastic epoxy (see Fig. 7). In early trials of this process, it was determined that heating temperature ramp rates in excess of 0.23°C/min resulted in alignment error due to phase change of the adhesive and subsequent drift of the microlens.

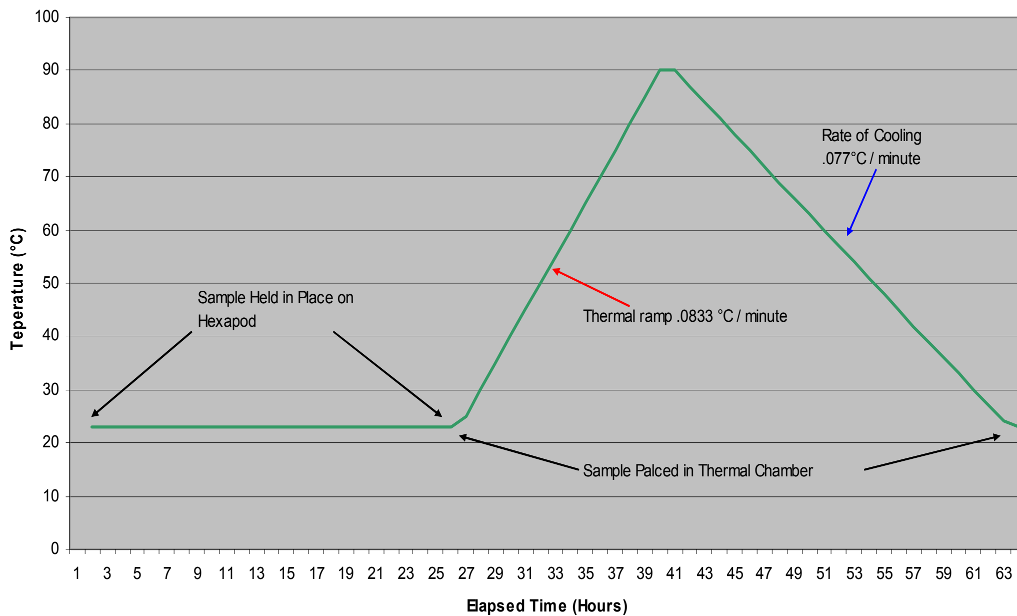


Figure 7. Example cure rate to achieve a Tg of 100°C for Tra-Con F-118 epoxy.

# 4. PACKAGING QUALIFICATION

For future DoD and NASA applications, the need exists for a qualification program that tests the existing packaged assembly to insure reliable operation of the APD FPA assembly. The package currently employed by MIT Lincoln Laboratory is a custom 160 Pin Grid Array (PGA) package manufactured by Kyocera (see Fig. 8). This package is designed to be hermetically sealed with an optically transparent window. Included in this design is a copper tungsten heat sink pedestal which allows for the removal of heat from the APD ROIC assembly.

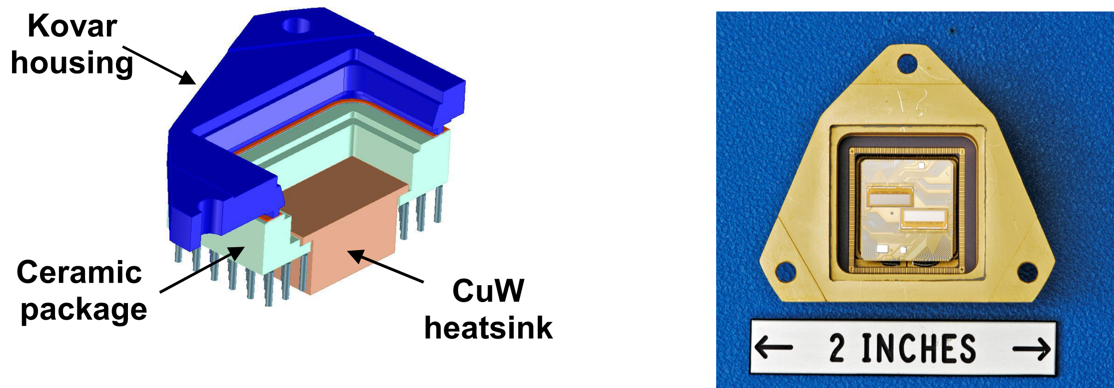


Figure 8. Cross sectional view and example of the 160 pin Kyocera APD package with a dual 128x32 APD arrays.

## 4.1 FPA Qualification Testing

MIT Lincoln Laboratory has been implementing a comprehensive component testing program, that involves a series of environmental tests designed to identify any issues related performance of the APD FPA packaged assembly. These studies include thermal, mechanical, environmental and electrical testing. Overall, the testing consisted of three segments of increasing stress exposure.

Three levels of testing were defined: acceptance, proto-flight and qualification, with each level designed to expose the packages to increasing environmental stressors. The test sequence involved measuring the baseline performance for each APD FPA package, which included detailed electrical measurements and high resolution photographs. Before and after each phase of testing, the performance metrics were again measured with the data correlated with the previous phase's results.

In a recently completed set of preliminary tests, four fully packaged FPAs were subjected to a subset of testing per MIL-STD-810F. For these tests, the 4 fully packaged APD FPAs were initially profiled for their baseline performance. The baseline testing looked at the overall electrical performance of the APD / ROIC assembly, the thermal performance of the Thermal Electric Cooler (TEC), the package hermeticity, and a thorough visual inspection of the gold bond wires and microlens assembly.

In measuring the electrical performance, the APD FPA was placed into a test fixture at which time ROIC-frame data was gathered and analyzed for overall performance and individual pixel functionality. The TEC performance was determined by measuring the dynamic impedance of the TEC and measuring the thermal performance of the TEC while under the operational heat load of the APD FPA (see Fig. 9). In the analysis of the TEC performance data after all exposure steps, it was found that there was no measurable difference in either the heat removal rate or the dynamic impedance measurements.

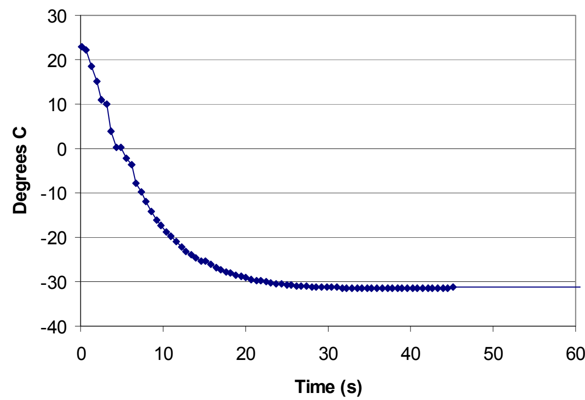


(a)

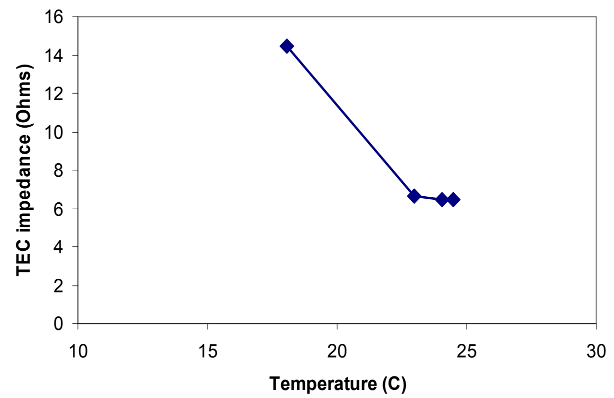


(b)

Figure. 9. Example TEC performance data for APD FPA package F4. *(a)* The post exposure thermal performance of the TEC while under nominal thermal load in package F4. This measures the TEC's ability to remove heat from the package within a given time period. *(b) R*esults of the dynamic impedance measurements that were made of the TEC at various operational temperatures.

Mechanical testing was performed using a three axes vibration table with the packages individually monitored on all three axes with localized accelerometers. During the testing, the mechanical stresses increased incrementally following a prescribed exposure profile (see Table 1). Before and after each exposure step, a white noise survey was taken for each individual axis (X, Y & Z) (see Fig. 10). Any substantial difference in these scans could indicate potential damage to the mechanical structure.

*Table 1*. Prescribed mechanical vibration exposure profile.

Acceleration Spectral Density **(ASD) g2/Hz**

| | **Acceptance** | **Protoflight** | **Qualification** |
|---|---|---|---|
| **Frequency (Hz)** | 60 Seconds | 120 Seconds | 240 Seconds |
| 20 | 0.0080 | 0.0160 | 0.0320 |
| 50 | 0.0500 | 0.1000 | 0.2000 |
| 125 | 0.0500 | 0.1000 | 0.2000 |
| 130 | 0.0125 | 0.0250 | 0.0500 |
| 1200 | 0.0125 | 0.0250 | 0.0500 |
| 2000 | 0.0045 | 0.0090 | 0.0180 |
| **Overall** | 4.90 grms | 6.90 grms | 9.80 grms |

Through all phases of testing (acceptance, proto-flight and qualification) no changes were observed either in the *in situ* data or white noise survey tests. It was noted that during the proto-flight testing that a cabling issue resulted in anomalies in the data that were later dismissed after resampling the white noise data and comparing it to the post acceptance level test data.

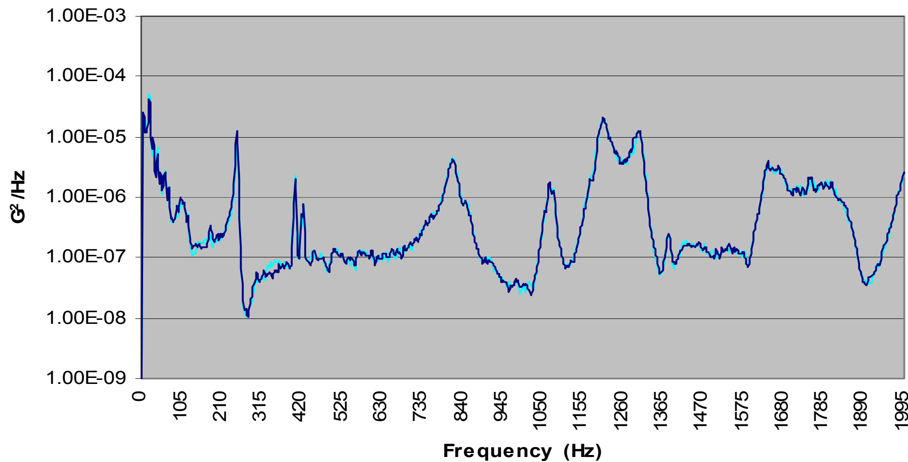


Figure 10. Package F4 pre & post Qualification exposure Y axis white noise sweeps.

This sweep is taken from 0.5Hz to 2 kHz with a magnitude of 0.5g.

# 5. CONCLUSIONS

While the efforts described above were successful, continued development in the areas of device screening, optical alignment and package qualification is expected to continue. Improvements in the microlens alignment techniques are also underway, which include the incorporation of the additional optics that are necessary to generate a particular cone angle for the incoming beam during the alignment process. This is expected to generate the alignment that best meets requirements of the front-end optics for a particular APD FPA system design.

# ACKNOWLEDGEMENT

This work has been sponsored by the U.S. Defense Advanced Research Project Agency under Air Force contract number FA8721-05-C-0002. The opinions, interpretations, conclusions, and recommendations are those of the authors and are not necessarily endorsed by the United States Government.

## REFERENCES

[1] S. Verghese, J.P. Donnelly, E.K. Duerr, K.A. McIntosh, D.C. Chapman, C.J. Vineis, G.M. Smith, J.E. Funk, K.E. Jensen, P.I. Hopman, D.C. Shaver, B.F. Aull, J.C. Aversa, J.P. Frechette, J.B. Glettler, Z.L. Liau, J.M. Mahan, L.J. Mahoney, K.M. Molvar, F.J. O'Donnell, D.C. Oakley, E.J. Ouellette, M.J. Renzi, and B.M. Tyrrell, "Arrays of InP-based Avalanche Photodiodes for Photon-Counting," *IEEE J. of Selected Topics in Quantum Electron.*, vol. 13, pp. 870-886, 2007.

[2] G.M. Smith, J.P. Donnelly, K.A. McIntosh, E.K. Duerr, D.C. Shaver, S. Verghese, J.E. Funk, N.R. Kumar, L.J. Mahoney, K.M. Molvar, F.J. O'Donnell, D.C. Chapman, D.C. Oakley, and K.G. Ray, "Design and reliability of mesa-etched InP-based Geiger-mode avalanche photodiodes," in IEEE LEOS Annual Meeting 2007 Technical Digest, WL1, 2007.